Noise-like pulse with a 690 fs pedestal generated from a nonlinear Yb-doped fiber amplification system

Zexin Zhang (张泽新)[1], Jinrong Tian (田金荣)[1,*], Changxing Xu (许昌兴)[1], Runqin Xu (徐润亲)[2], Youshuo Cui (崔友硕)[1], Bihui Zhuang (庄碧辉)[1], and Yanrong Song (宋晏蓉)[1]

[1]*College of Physics and Optoelectronics, Faculty of Science, Beijing University of Technology, Beijing 100124, China*
[2]*Institute of Automation, Chinese Academy of Sciences, Beijing 100190, China*
**Corresponding author: jrtian@bjut.edu.cn*

Received July 16, 2020; accepted September 11, 2020; posted online October 23, 2020

Noise-like pulses having a pedestal of 690 fs and a spike of 59.6 fs were generated in a nonlinear Yb-doped fiber amplification system. The seed source is a mode-locked Yb-doped fiber laser by nonlinear polarization rotation, and dissipative soliton pulses were obtained in it. Then, the dissipative soliton pulses passed through a 7.6 m dispersive fiber to enhance the dispersion and nonlinearity. Further on, the dissipative soliton pulses were launched into a Yb-doped fiber nonlinear amplifier, and stable noise-like pulses with a pedestal of 6.26 ps and a spike of 227 fs were achieved. Finally, by a grating pair, the pedestal and spike of the noise-like pulses were effectively compressed to 690 fs and 59.6 fs, respectively. To the best of our knowledge, this is the shortest pedestal demonstrated in noise-like pulses operating at 1 μm.

Keywords: fiber laser; amplifier; compression; noise-like pulse.
doi: 10.3788/COL202018.121403.

Ultrafast fiber lasers have attracted much attention due to potential applications in optical communication, remote sensing, micro-machining, medical treatment[1–3], etc. The pulses generated in ultrafast fiber lasers have desirable characteristics such as ultra-short duration, high peak power, and broadband spectrum, which entails the implementation of mode-locking techniques for the generation of picosecond or femtosecond pulses. Over the past few decades, researchers have explored different types of mode-locking techniques such as solitons, similaritons, and dissipative solitons (DSs). However, pulse energy scaling for these kinds of pulses is usually limited by nonlinear effects or damage threshold. Thus, the noise-like pulse (NLP), reported first, to the best of our knowledge, in 1997[4], has been receiving an increasing amount of attention due to its great potential in higher energy pulse generation.

In the past few years, extensive investigations on NLPs have been presented. Typically, an NLP is composed of wave-packets with a fine inner structure of sub-pulses that have stochastically varying durations and peak intensities[5] because of fiber birefringence[4], nonlinear instability[6], soliton collapsing[7], or the peak power clamping effect[8]. This temporal feature gives rise to a double-scaled autocorrelation trace with a spike riding upon a wide and smooth pedestal, which implies a low temporal coherence. Therefore, NLPs may find various applications in optical metrology, optical sensing[9,10], optical coherence tomography, optical communication[11,12], and industrial micro-machining[13,14], with a favorable combination of low temporal coherence and high pulse energy. A number of measures can be implemented to obtain NLPs in fiber lasers, such as mode locking by nonlinear polarization rotation (NPR)[15–19], nonlinear optical loop mirror[20–22], nonlinear amplifying loop mirror[23,24], semiconductor saturable absorption mirror[25], or other saturable absorber materials[26–28]. Since the first, to the best of our knowledge, demonstration in 1997[4], the NLP's pulse duration has been of great interest because of the difficulty in its compression. The shortest pulse duration of the pedestal and spike are 920 fs[29] and 14.3 fs[24], respectively, in the wavelength region around 1 μm.

In this Letter, we demonstrated generation and compression of NLPs in a nonlinear Yb-doped fiber amplification system in experiment. The DS pulse from an NPR mode-locked fiber laser passed a 7.6 m dispersive fiber to enhance the dispersion and nonlinearity. After amplification in a nonlinear Yb-doped fiber amplifier, stable NLPs with a pedestal of 6.26 ps and a spike of 227 fs were achieved. The NLPs were further compressed by a grating pair, and the pedestal and spike were compressed to 690 fs and 59.6 fs, respectively. To the best of our knowledge, this is the shortest pedestal of the NLPs operating at 1 μm.

The experimental setup is depicted in Fig. 1, which is composed of an oscillator, an amplifier, and a compressor. Figure 1(a) shows the oscillator, which is an NPR mode-locked all-normal-dispersion Yb-doped fiber laser pumped by a laser diode with output power up to 600 mW. In the fiber laser, two collimators (C1 and C2) are separated by 20 cm. The 3 dB bandwidth of the birefringence filter (BF) is 12 nm, and a 70:30 output coupler (OC) at 1 μm is used to couple laser out. The optical isolator (ISO) forces unidirectional operation. Figure 1(b) illustrates the nonlinear Yb-doped fiber amplifier. Different from our previous work[29], a 7.6 m single mode fiber (SMF28) is inserted between the ISO and the combiner as the dispersive fiber to

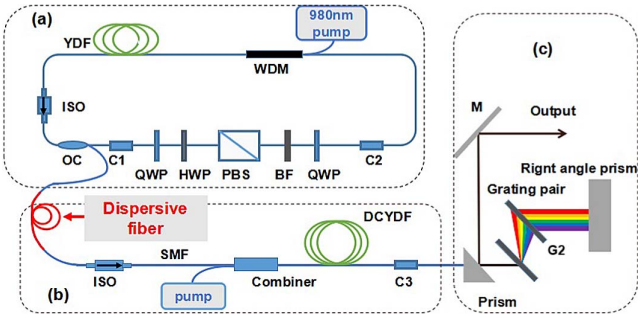

Fig. 1. Schematic of the nonlinear Yb-doped fiber amplified system. (a) Oscillator, (b) amplifier, and (c) compressor. WDM, wavelength division multiplexer; YDF, Yb-doped fiber; ISO, isolator; OC, output coupler; QWP, quarter-wave plate; HWP, half-wave plate; PBS, polarized beam splitter; BF, birefringence filter; DCYDF, double-cladding Yb-doped fiber; C1–C3, collimators; M, high reflection mirror.

balance the dispersion and nonlinearity of the system. To facilitate the generation of NLPs in the amplifier, a 5.3 m double-cladding Yb-doped gain fiber (LMA-YDF-10/130 VIII, Nufern) is chosen for high gain, which is forward-pumped by a diode laser with output power up to 9 W. Figure 1(c) shows the compressor consisting of a grating pair, two prisms, and a high reflective mirror. The counter propagating beams are slightly off-set spatially to guide the laser beam out after compression. The groove density of each grating is 1000 lines/mm (LSFSG-1000-1010-94, LightSmyth).

The mode locking of the fiber laser was self-started, and its output could be switched from a DS pulse to an NLP by simply increasing the pump power in the experiment. In contrast with our previous work[29], a lower mode-locking threshold and more stable pulse could be obtained by adjusting the tilt angle of the optics such as a quarter-wave plate, half-wave plate, and BF. Considering the stability and compressibility, the oscillator is operating in the regime of the DS pulse rather than the NLP. The output characteristics are demonstrated in Fig. 2. Figure 2(a) shows the spectral evolution, in which the center wavelength was approximately 1030 nm, and the 3 dB spectral bandwidth was 15 nm (Yokogawa, AQ6370C). Figure 2(b) shows the RF spectrum (Agilent E4447A), and a repetition rate of 37.48 MHz could be derived from

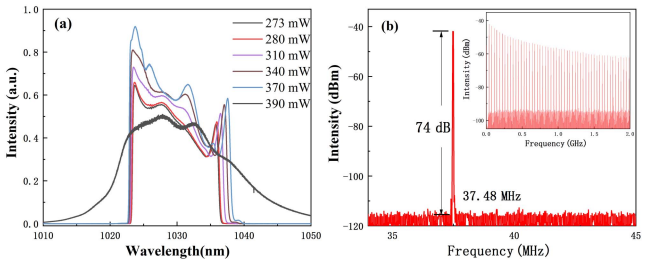

Fig. 2. Output characteristics of the oscillator. (a) Spectral emission versus pump power. (b) RF spectrum (34–45 MHz). Inset: RF spectrum in the span of 2 GHz.

it. The signal-to-noise ratio (SNR) was about 74 dB, which indicated that the mode locking was very stable.

Considering the tradeoff of stability and spectrum, the oscillator operated at the pump power of 340 mW, while the output power was 32 mW. The output pulse from the oscillator propagated in a 7.6 m dispersive SMF to enhance the dispersion and nonlinearity and was launched into the amplifier. In the amplifier, the intensity and phase structure of the DS pulse had been greatly changed by the nonlinear effects such as self-phase modulation, cross-phase modulation, stimulated Raman scattering, etc. due to the high peak power laser; finally, the DS pulse transformed into an NLP, and the mechanism of this evolution had been explained theoretically and confirmed in previous work[24]. Figure 3 shows the spectrum of the output pulse at pump power from 1 W to 9 W. With the increase of pump power, the Raman component began to appear due to the nonlinear effects during the process of amplification. When the pump power was increased to 3 W, the first-order Raman component started to become noticeable (~1077 nm). On further increase of the pump power, one might observe the first-order Raman component gradually increased and became strongest at a pump power of 5 W, while the second-order Raman component appeared. When the pump power exceeded 7 W, the second-order Raman component was obviously noticeable, and the spectrum is flat and broad.

The output power of amplified pulses was measured (Newport 1916-C) and depicted in Fig. 4. The maximum output power of 5.08 W was achieved at a pump power of 9 W, and the slope efficiency was approximately 56.4%, which indicated the high conversion efficiency of the amplifier. The single pulse energy was calculated to be about 136 nJ.

The NLP generated through the amplification system was compressed by a compressor shown in Fig. 1(c), where the second grating (G2) was mounted on a two-axis translation stage allowing for both fine tuning of the position of G2 and adjusting the separation of the grating pair over long distances. Since the diffractive spectrum was very

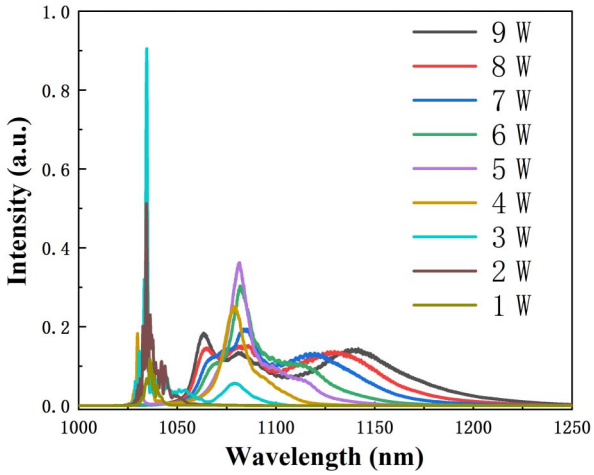

Fig. 3. Spectrum of the amplified pulse with respect to pump power.

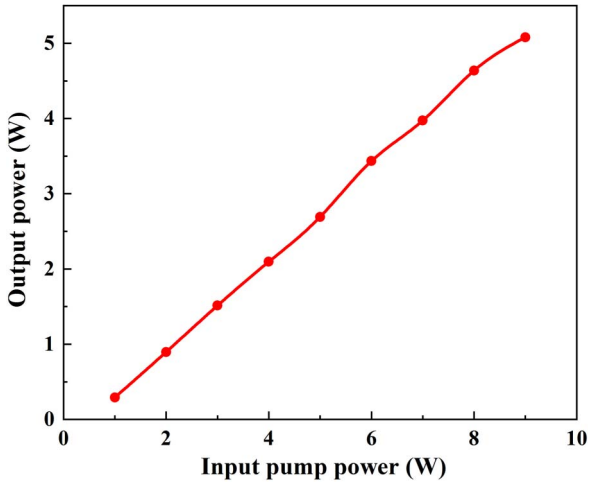

Fig. 4. Output power of the amplifier as a function of pump power.

broad beyond the capacity of the grating, thus part of it had to be abandoned. So, the grating pair could be used both as a spectral filter and compressor. To check the effect of the grating pair compressor, the pulse duration was determined by autocorrelation measurement (FR103-XL, FEMTOCHROME). At a fixed pump power, the autocorrelation traces with respect to the separation of two gratings were recorded, and the pulse duration of the pedestal and spike was deduced with an assumed Gaussian pulse. Figure 5 shows the result, in which both the pulse duration of the pedestal and spike experienced a successive decrease and increase with respect to the separation of the grating pair, which justified the effectiveness of the grating pair. However, the difficulty in compressing NLPs manifested itself in the very slow varying pulse duration, which is attributed to the complex dispersive and spectral structure rather than DSs and normal solitons. Therefore, proper spectral shaping was necessary to obtain shorter NLPs.

Spectral shaping of NLPs could be implemented by the change of pump power and adjusting the position of the grating. The aforementioned dependence of the spectrum on pump power shown in Fig. 3 had shown that the broadest spectrum was obtained at a pump power of 8–9 W. Thus, we increased the pump power of the amplifier gradually from 7.6 W to 8.6 W for the most suitable pump power. At each pump power, the grating pair was finely tuned to obtain the shortest pulse, and autocorrelation trace was recorded. Figure 6(a) shows the trend of the shortest pulse duration at each pump power from 7.6 W to 8.6 W in steps of 0.2 W, where the asymmetry of the curve is caused by the imbalance of the diffraction loss and compression ability of the grating pair, and it generally conforms to the compression law. The autocorrelation traces of the NLP at pump power of 8 W are shown in Fig. 6(b). In contrast with common NLPs, these autocorrelation traces had nearly a smooth profile, and there was no obvious boundary between the spike and the pedestal due to the overlap between the top of the pedestal and the bottom of the spike. From Fig. 6(b), the NLP has a 690 fs pedestal and a 59.6 fs spike, which is the shortest pedestal for NLPs operating at 1 μm to date.

To obtain the compression ratio, the autocorrelation trace at the pump power of 8 W was measured before compression and shown in Fig. 7, in which the pulse duration

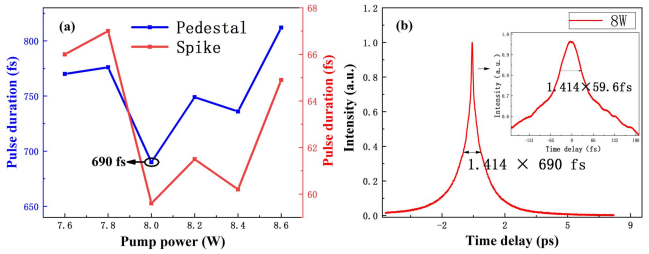

Fig. 6. (a) Shortest pulse duration of a compressed NLP at different pump powers (7.6–8.6 W). (b) Autocorrelation traces of an NLP at pump power of 8 W. Inset: the corresponding spike.

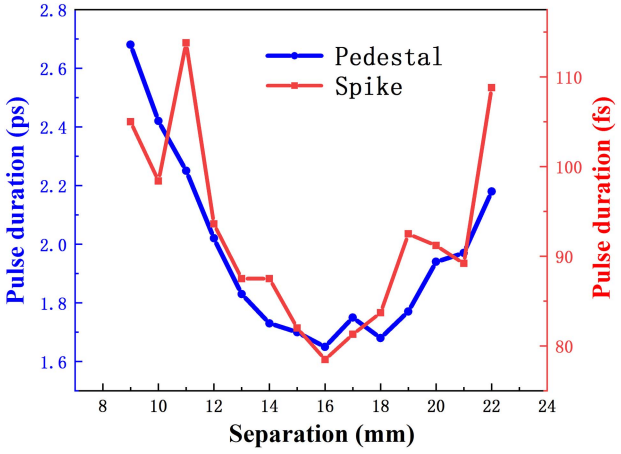

Fig. 5. Pulse duration of the NLPs as a function of separation of the grating pair (red line, pedestal; blue line, spike).

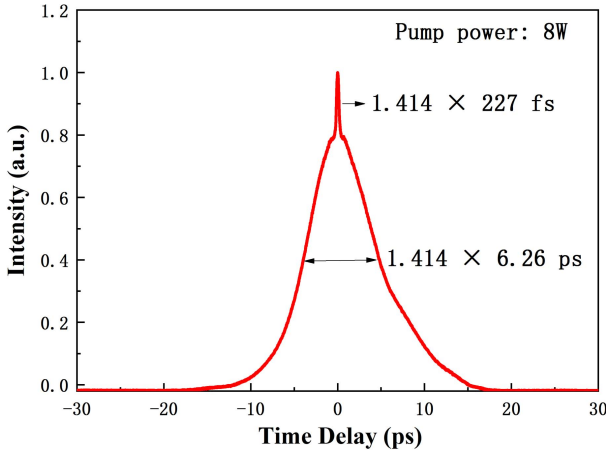

Fig. 7. Autocorrelation trace of the NLP at a pump power of 8 W before compression.

of the pedestal and spike was 6.26 ps and 227 fs, respectively. Compared to the pulse width of 690 fs and 59.6 fs after compression, the NLP was obviously compressed. Furthermore, it was noteworthy that the compression ratio of the pedestal and spike was not equal, which was attributed to the spike corresponding to more frequencies, and the dispersion compensation was more rigorous than the pedestal.

To better understand the spectral effect of compression, we measured the spectra while increasing the pump power from 1 W to 9 W in steps of 1 W after compression, and Fig. 8 shows the result. Compared with the counterpart before compression, the spectrum was significantly tailored at the pump power from 7 W to 9 W, and the energy was concentrated on around the laser line, while the Raman components are drastically weakened due to the filter effect of the grating pair. In combination with Fig. 5, it can be concluded that both spectral shaping and dispersion of the grating pair contributed to shortening of the NLP's pulse width.

The output power after compression is shown in Fig. 9, which has an abrupt fall attributed to the spectral filtering of the grating pair. Although the fiber amplifier yielded 4.636 W average power at pump power of 8 W, the output power was only 282 mW (corresponding to the single pulse energy of 7.5 nJ and the peak power of 10.9 kW) after compression, which was attributed to the abandoning of quite a few spectral components. As a result, the output power suffered a severe loss, which remained a problem for the compression of NLPs. In spite of this, it was a valuable attempt to obtain the shortest NLP, and the moderate pedestal could possibly enable linear amplification to increase the pulse energy while keeping the pulse duration almost unchanged for NLPs.

Figure 10 shows the RF spectrum at pump power of 8 W after compression. The repetition rate was the same 37.48 MHz as that of the oscillator. Due to the high scanning resolution and small pulse time jitter, the RF spectrum does not contain a typical noise pedestal present in NLPs. Although passing through a complex optical path in the amplifier and compressor, the output NLP had an SNR of 62 dB, which demonstrated that the pulse was still very stable after compression.

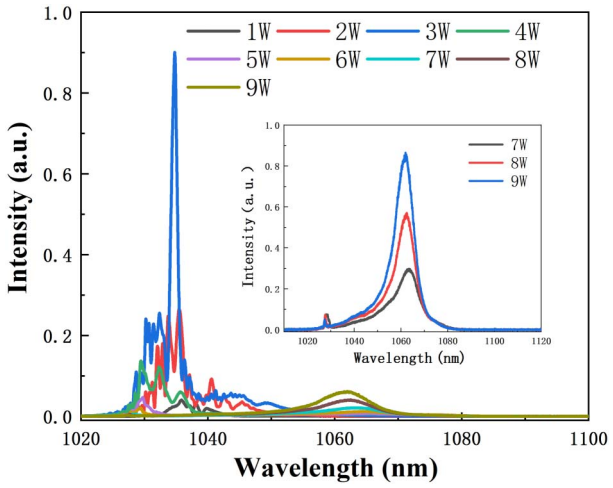

Fig. 8. Spectrum versus the pump power after compression. Inset: spectrum at pump power of 7–9 W.

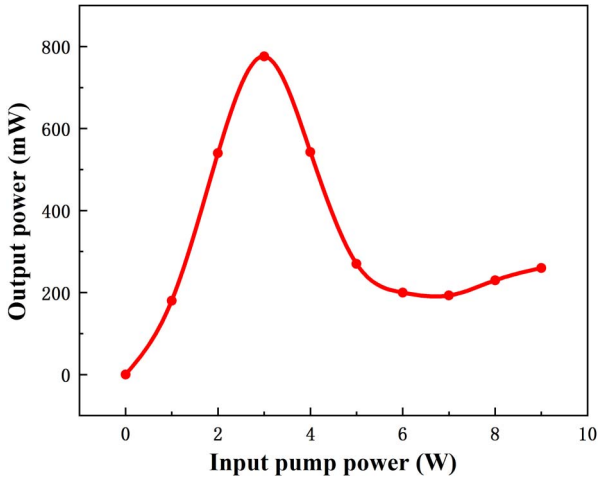

Fig. 9. Output power with respect to pump power after compression.

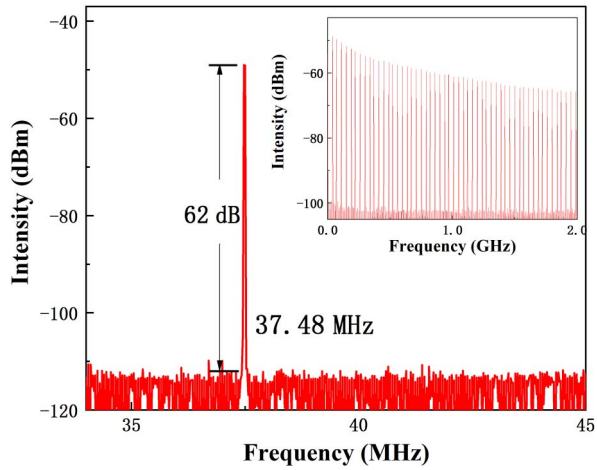

Fig. 10. RF spectrum of the NLP from 34 to 45 MHz after compression. Inset: RF spectrum in the span of 2 GHz.

In summary, we demonstrated the generation and compression of an NLP in a fiber laser amplifier system experimentally. The laser system included an NPR mode-locked Yb-doped fiber laser, a Yb-doped fiber amplifier, and a compressor. We inserted a 7.6 m dispersive fiber between the oscillator and the amplifier to enhance the dispersion and nonlinearity for the first time, to the best of our knowledge, in the compression of NLPs. Finally, an NLP with a 690 fs pedestal and a 59.6 fs spike was obtained at 1062 nm. To the best of our knowledge, this is the shortest pedestal of NLPs operating in the wavelength region around 1 μm. We think that this laser may find its applications in optical coherence tomography, supercontinuum generation, micromachining, and other fields.

This work was supported by the Beijing Natural Science Foundation (No. 4192015) and the National Natural Science Foundation of China (No. 61975003).

References

1. U. Keller, Nature **424**, 831 (2003).
2. M. E. Fermann and I. Hartl, Nat. Photon. **7**, 868 (2013).
3. H. Ahmad, S. N. Aidit, S. I. Ooi, and C. Tiu, Chin. Opt. Lett. **16**, 121405 (2018).
4. M. Horowitz, Y. Barad, and Y. Silberberg, Opt. Lett. **22**, 799 (1997).
5. S. S. Lin, S. K. Hwang, and J. M. Liu, Opt. Express **22**, 4152 (2014).
6. S. Kobtsev, S. Kukarin, S. Smirnov, S. Turitsyn, and A. Latkin, Opt. Express **17**, 20707 (2009).
7. D. Y. Tang, L. M. Zhao, and B. Zhao, Opt. Express **13**, 2289 (2005).
8. L. M. Zhao, D. Y. Tang, J. Wu, X. Q. Fu, and S. C. Wen, Opt. Express **15**, 2145 (2007).
9. M. A. Putnam, M. L. Dennis, I. N. Duling, C. G. Askin, and E. J. Friebele, Opt. Lett. **23**, 138 (1998).
10. V. Goloborodko, S. Keren, A. Rosenthal, B. Levit, and M. Horowitz, Appl. Opt. **42**, 2284 (2003).
11. S. Keren and M. Horowitz, Opt. Lett. **26**, 328 (2001).
12. S. Keren, E. Brand, Y. Levi, B. Levit, and M. Horowitz, Opt. Lett. **27**, 125 (2002).
13. V. Agrez and R. Petkovsek, Appl. Opt. **52**, 3066 (2013).
14. K. Ozgoren, B. Oktem, S. Yilmaz, F. O. Ilday, and K. Eken, Opt. Express **19**, 17647 (2011).
15. X. L. Li, S. M. Zhang, M. M. Han, and J. M. Liu, Opt. Lett. **42**, 4203 (2017).
16. J. H. Lin, C. L. Chen, C. W. Chan, W. C. Chang, and Y. H. Chen, Opt. Lett. **41**, 5310 (2016).
17. T. North and M. Rochette, Opt. Lett. **38**, 890 (2013).
18. H. Ahmad, S. I. Ooi, M. Z. A. Razak, S. R. Azzuhri, A. A. Jasim, K. Thambiratnam, M. F. Ismail, and M. A. Ismail, Chin. Opt. Lett. **15**, 051402 (2017).
19. Q. Wang, T. Chen, B. Zhang, A. P. Heberle, and K. P. Chen, Opt. Lett. **36**, 3750 (2011).
20. J. F. Li, Z. X. Zhang, Z. Y. Sun, H. Y. Luo, Y. Liu, Z. J. Yan, C. B. Mou, L. Zhang, and S. K. Turitsyn, Opt. Express **22**, 7875 (2014).
21. J. K. Shi, Y. Li, S. Y. Gao, Y. L. Pan, G. M. Wang, R. Y. Ji, and W. H. Zhou, Chin. Opt. Lett. **16**, 121404 (2018).
22. O. Pottiez, R. Paez-Aguirre, J. L. Cruz, M. V. Andres, and E. A. Kuzin, Opt. Commun. **377**, 41 (2016).
23. S. Liu, F. P. Yan, L. N. Zhang, W. G. Han, Z. Y. Bai, and H. Zhou, J. Opt. **18**, 015508 (2016).
24. R. Q. Xu, J. R. Tian, and Y. R. Song, Opt. Lett. **43**, 1910 (2018).
25. Y. Mashiko, E. Fujita, and M. Tokurakawa, Opt. Express. **24**, 26515 (2016).
26. Y. D. Cui, J. Opt. **18**, 105503 (2016).
27. R. L. Miao, M. Y. Tong, K. Yin, H. Ouyang, Z. Y. Wang, X. Zheng, X. A. Cheng, and T. Jiang, Chin. Opt. Lett. **17**, 071403 (2019).
28. W. P. Zhang, Y. R. Song, H. Y. Guoyu, R. Q. Xu, Z. K. Dong, K. X. Li, J. R. Tian, and S. Gong, Opt. Eng. **56**, 126101 (2017).
29. C. X. Xu, J. R. Tian, R. Q. Xu, Y. F. Wu, L. Y. Fan, J. Y. Guo, and Y. R. Song, Opt. Express **27**, 1208 (2019).